Journal of Alloys and Compounds 747 (2018) 636–639

Contents lists available at ScienceDirect

Journal of Alloys and Compounds

journal homepage: http://www.elsevier.com/locate/jalcom

Structures and physical properties of two magnetic Fe-based metallic glasses

Jiliang Zhang [a, b], Guangcun Shan [a, b, *], Jiong Li [c], Yingmin Wang [d], Chan Hung Shek [b, **]

[a] School of Instrument Science and Opto-electronics Engineering, Institute of Precision Instrument and Quantum Sensing, Beihang University, Beijing 100191, China
[b] Department of Physics and Materials Science, City University of Hong Kong, Kowloon Tong, Hong Kong Special Administrative Region
[c] Shanghai Synchrotron Radiation Facility, Shanghai Institute of Applied Physics, Shanghai 200624, PR China
[d] Key Laboratory of Materials Modification by Laser, Ion, and Electron Beams, Ministry of Education, School of Materials Science and Engineering, Dalian University of Technology, Dalian 116024, PR China

ARTICLE INFO

Article history:
Received 10 January 2018
Received in revised form
6 March 2018
Accepted 8 March 2018
Available online 9 March 2018

Keywords:
Metallic glass
Magnetic
Atomic cluster
Structure
EXAFS

ABSTRACT

Significant differences in structural, thermal, mechanical and magnetic properties were observed between traditional FeSiB metallic glass and newly developed FeMB (M = mixture of Zr, Nb and Y) metallic glass. The origin of the differences is attributed to the more negative heat of mixing between boron and the metallic alloying elements. This leads to the transition of local structure and bonding nature of Fe–B elucidated by the measured extended X-ray absorption fine structure (EXAFS) spectra functions that were analyzed employing *ab initio* multiple scattering calculations using the FEFF8.4 code and by the electronic structures of Fe as well. Such dramatic change sheds light on the understanding of the correlations between structure and physical properties in metallic glasses. The results were discussed based on electronic structures and they provide a new route to design magnetic Fe-based metallic glasses.
© 2018 Elsevier B.V. All rights reserved.

1. Introduction

FeB-based metallic glass were extensively investigated because of the wide applications in electrical transformers, magnetic sensors and radio-frequency inductive devices, etc. due to their many advantages compared with traditional silicon steels [1–3]. In recent years, several families of Fe-based metallic glasses with high glass forming ability (GFA) were developed [4–6]. Nevertheless, most of these new members exhibit poor soft magnetic behaviors and some even show no ferromagnetic behavior at room temperature. It is therefore vital to understand the structural nature which gives rise to their magnetic properties.

The stereochemically defined model stipulates that local unit with nearest neighbors in metal-metalloid metallic glasses has the same type of structure and composition as their crystalline counterparts [7], which provides a good description of the structural properties of tradition metals-metalloid metallic glasses. Recently, Zhang et al. [8,9] developed two kinds of CoSiB metallic glasses with distinct magnetic properties based on different local unit in intermetallics, despite their similar compositions. The newly developed metallic glasses of large GFA show dominant unit of icosahedral clusters bridged by minor clusters or atoms [10–13]. Such different local structures likely gave rise to different magnetic behaviors in Fe-based metallic glasses, since magnetic moment is predominantly a localized phenomenon. In this study, we investigated the structure and properties of two FeB-based metallic glasses with significantly different GFA, namely $Fe_{71}B_{17}Si_{12}$ (FeBSi) and $Fe_{71}B_{17}Nb_4Y_4Zr_4$ (FeBM) respectively, and explored the correlations among the local order and properties.

2. Experiments

Master ingots of the two nominal compositions as well as $Fe_{80}B_{20}$ were prepared by arc melting the mixtures of pure constituent elements Fe (99.99 wt%), B (99.9 wt%), Si (99.99 wt%), Nb (99.9 wt%), Y (99.9 wt%) and Zr (99.9 wt%) under a Ti-gettered argon atmosphere. Using these master ingots, ribbon samples

* Corresponding author. School of Instrument Science and Opto-electronics Engineering & Institute of Precision Instrument and Quantum Sensing, Beihang University, Beijing 100191, China.
** Corresponding author.
E-mail addresses: gshan2-c@my.cityu.edu.hk (G. Shan), apchshek@cityu.edu.hk (C.H. Shek).

https://doi.org/10.1016/j.jallcom.2018.03.085
0925-8388/© 2018 Elsevier B.V. All rights reserved.

with thickness of ~30 μm and width of ~2 mm were produced by a single roller melt-spinning apparatus. Structural identification was conducted on a Philips X'pert X-ray diffractometer (Cu Kα, λ = 0.15406 nm). Thermal stability was measured with a Perkin Elmer Diamond differential scanning calorimeter (DSC) at a heating rate of 20 K/min. Magnetic measurements were carried out using a Cryogenic vibrating sample magnetometer with a maximum field of up to 50000 Oe. Domain structures of ribbons were observed with a Vecco magnetic force microscope (MFM) operated in the tapping/lift scanning mode. Electronic structure was measured using x-ray photoelectron spectroscopy (XPS) with a monochromatized Al K_α radiation (1486.6 eV) in an ULVAC-PHI 5802 system (Kanagawa, Japan). The atomic-scale structures of these metallic glasses were investigated by EXAFS spectroscopy at beam line BL14W of the Shanghai synchrotron radiation facility, Shanghai, China. EXAFS spectra of Fe–K edge was measured in transmission mode at temperature 300 ± 2 K. The thicknesses of the samples were optimized to obtain suitable absorption jumps at each K-absorption edge. The experimental EXAFS signals were extracted by a standard data-reduction procedure using the Athena program [14]. Note that the EXAFS spectra model of the simulated atomic configurations were fitted using an *ab initio* multiple scattering calculation implemented in FEFF8.4 [15].

3. Results and discussions

XRD patterns in Fig. 1 confirmed the glassy nature of both samples. A side-by-side comparison of XRD patterns for the two metallic glasses shows that the diffuse hump in the FeBM metallic glasses is not only broadened, but shifted towards smaller angle as well. The difference is made evident by the Gaussian fitting on the peaks (see solid lines in Fig. 1). It suggests more variation of the local structure in FeBM metallic glasses. Because pair distribution function (PDF) is a Fourier sine transform of powder XRD (after the corrections of instrumental sources and backgrounds), the shift of the amorphous hump towards low angle in the XRD pattern of the FeBM metallic glass indicates that it has a larger dominant nearest neighboring distance, while the broadening profile suggests more different atomic clusters from the dominant nearest neighboring distances in the FeBM metallic glass. Like most FeBSi metallic glasses, the present FeBSi metallic glass did not exhibit a detectable glass transition in the DSC scans [16]. Its crystallization temperature T_x was 851 K, which was typical for traditional FeBSi metallic glasses [1]. The FeBM metallic glasses show high thermal stability with $T_g = 873$ K and $T_x = 922$ K, which were the same as the reported values [7]. The addition of transition metals yields high GFA and high thermal stability, viz., 71 K higher than FeBSi in crystallization temperature. Such large difference of thermal stability is not common in metallic glasses based on one primary element. In Zr–Al-TM systems, there is only 30 K difference in crystallization temperature when the concentration of Zr changes from less than 55% to more than 65% [2,13]. Such obvious change can be explained in terms of local structures, as discussed previously for CoBSi metallic glasses [8]. Significant differences should be expected in its properties, especially in magnetic behaviors.

The nanoindentation load-penetration curves revealed distinctive mechanical behaviors of the two types of metallic glasses (see Fig. 2). The FeBSi metallic glass shows a higher hardness and larger elastic modulus, despite its lower thermal stability. Such mechanical behaviors are different from that expected normally, and this may suggest that the local structural units in these two metallic glasses are completely different. The dramatic change of such mechanical properties is not common in minor alloyed metallic glasses [1,2,13]. This supports that the difference should be related to distinctive structural change and even the change in bonding nature.

The magnetization curves in Fig. 3 show the magnetic behaviors of the two metallic glasses. Both metallic glasses show high initial magnetic susceptibility and small magnetic hysteresis, which are favorable for soft magnetic materials. It seems that these soft magnetic characters including high initial susceptibility and low coercive force are not affected significantly by the change of local structure but related to the amorphous state. The main difference is the much smaller saturation magnetization of the FeBM compared with that of FeBSi. The large initial susceptibility and small saturation field suggest that the small saturation moment in the latter should not be an indication of antiferromagnetic order but from reduced net spin per atom due to the local structure.

To clarify such change from the perspective of local structures, the EXAFS technique was employed. The Fourier transform of the experimental EXAFS spectra $K^2\chi(K)$ of FeBSi and FeBM glassy alloys, i.e., $\chi(R)$, at Fe–K edges exhibit evident differences, as shown in Fig. 4. The parameter K is the wave number of the photoelectron in XAFS process, which has dimensions of 1/distance, and is defined as

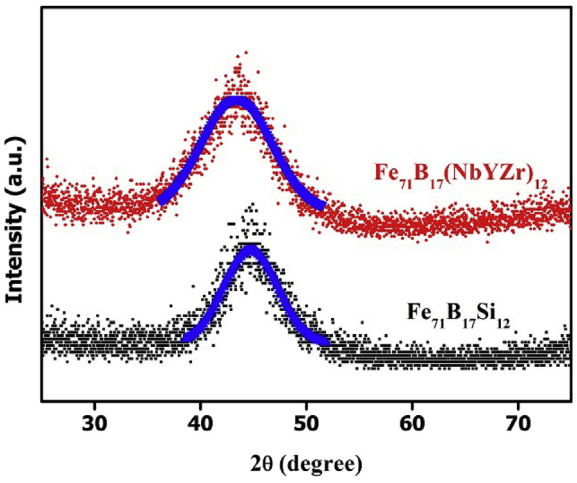

Fig. 1. XRD patterns of two Fe-based metallic glasses. The solid lines show the Gaussian fittings.

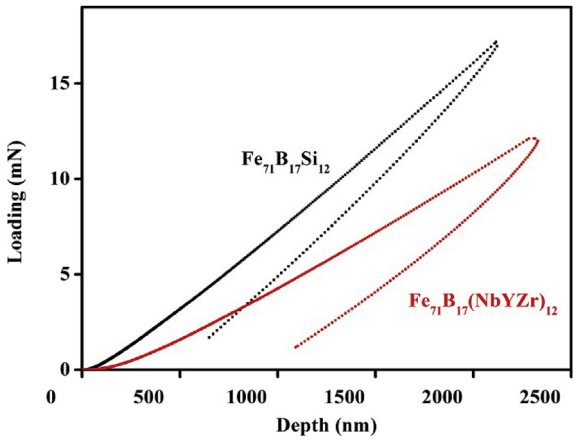

Fig. 2. Load-penetration curves of two Fe-based metallic glasses obtained with nanoindentation.

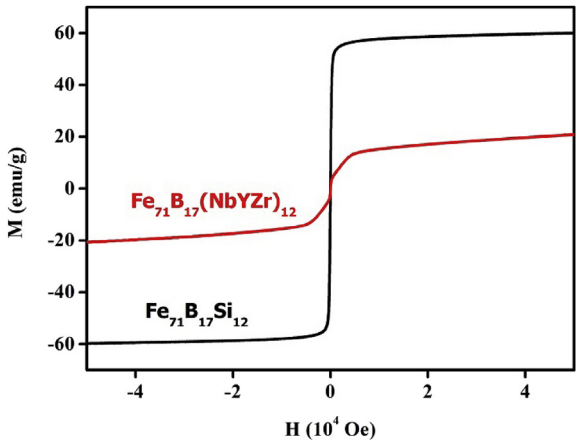

Fig. 3. Room-temperature magnetizations of two Fe-based metallic glasses.

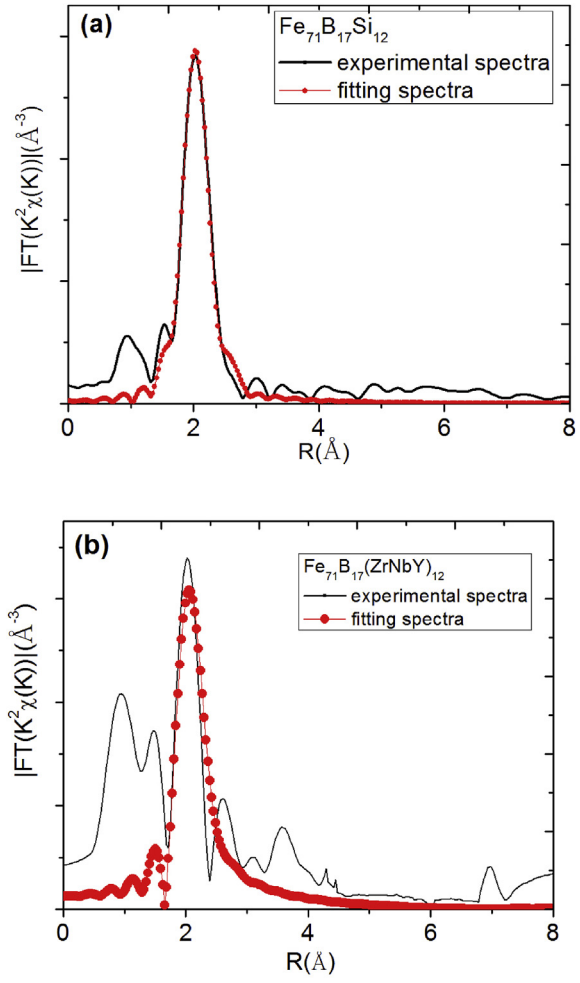

FIG 4

Fig. 4. Fourier transforms of the experimental EXAFS spectra $FT[K^2\chi(K)]$ of two Fe-based metallic glasses.

$$K = \frac{\sqrt{2m(E - E_0)}}{\hbar} \quad (1)$$

where E_0 is the absorption K-edge energy of the Fe element, E is the incoming X-ray energy from the synchrotron source and m is the electron mass. Obviously, the EXAFS results of FeBSi sample exhibited a stronger peak than that of FeBM sample. Compared to FeBM, the experimental EXAFS result of which shows a broad SRO peak, there are stronger short range order (SRO) peak and also a pretty clear medium range order (MRO) peak as well in FeBSi as seen from Fig. 4. In the range from 1 Å to 3 Å, there is one peak located at around 2.01 Å with a shoulder at around 2.6 Å in FeBSi, while there is a broad one peak at 2.05 Å with a shoulder at around 2.8 Å in FeBM. The integration area of the broad peak for FeBSi is much larger than that for FeBM. Considering the identical Fe and B contents in the two metallic glasses, it can be inferred that the FeBM has a higher coordination number (CN) in the first shell. Since nanocrystallization of FeBSi metallic glass is characterized by the presence of a dominant peak at 4.5 Å [17], the FeBSi metallic glass should be free of nanocrystals. According to the dense random packing model, there are five types of clusters, which are extracted from their crystalline counterparts, in conventional transition metal-metalloid metallic glasses [18]. It is therefore reasonable for such metallic glasses to show strong SRO and even MRO with low coordination number, compared with the bulk metallic glasses, in which icosahedral clusters generally dominate [19]. The addition of Y, Zr and Nb destroys the strong SRO and yields the icosahedral cluster due to their bigger atomic sizes or higher number of valence electrons. Obviously the destruction of strong SROs and MROs in FeBM will favor a high glass forming ability. It has been reported that the regions of MRO act as nucleation sites for α-Fe nanocrystals in Fe-based metallic glasses [20].

To understand the correlations among the local structures and physical properties, XPS was employed to inspect the electronic structure of the two metallic glasses, because of its sensitivity to the local structure, as well as its direct correlation to GFA and many other properties [21,22]. The electronic structures around Fermi level of the metallic glasses are shown in Fig. 5. The FeBM metallic glasses show three obviously different characteristics from those of traditional FeB or FeBSi metallic glasses, namely: 1) absence of the small peak around 9 eV; 2) absence of the shoulder next to the main peak; 3) peak shift towards lower energy around the Fermi level. The lower-energy binding state makes the FeBM metallic glasses more stable compared with FeBSi. However, the lower-energy binding state also resulted in overlapping of the shoulder and main peak. The shoulder corresponds to the minor bands of 3 d electrons whilst the main peak corresponds to the major bands [23]. The absence of the shoulder and shift of the peak indicates

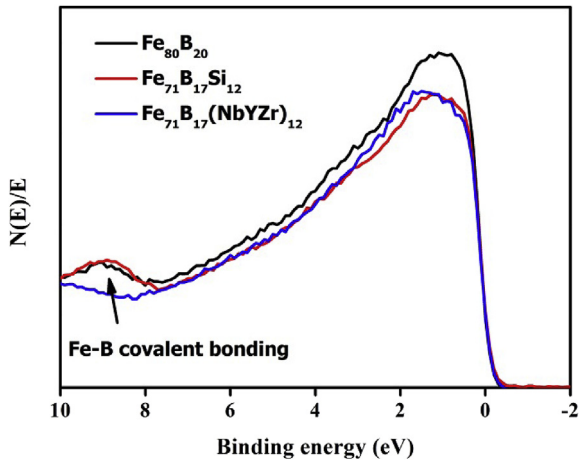

Fig. 5. Electronic structures obtained from XPS measurements: FeB metallic glass is a reference here.

that more electrons were transferred into minor bands, which reduced the net spins and thus led to a smaller magnetic moment. Such electronic structures provide insights to design of Fe-based magnetic metallic glasses. For a good ferromagnetic metallic glass, one should balance between GFA and magnetic behaviors by lowering the energy of binding state while avoiding electron transfer from major bands to minor bands.

The peak around 9 eV indicates the strong hybridization of B 2p and Fe 3 d bands, via the formation of Fe–B covalent-like bonds [23], which gives rise to the high hardness and elastic modulus in FeBSi metallic glasses as shown in Fig. 2. However, the low thermal stability suggests that the glass transition and crystallization in FeBSi metallic glasses does not involve extensive breaking of Fe–B covalent bonds, because of the much higher bond energy of a covalent bond than that of a metallic bond. This interpretation is also supported by the existence of the hybridization peak of B 2p and Fe 3 d bands in crystalline Fe_2B, the main crystallization product of the FeBSi metallic glasses [24], and the similarity in local structure between FeBSi metallic glasses and their crystalline counterparts.

The phenomenon also reveals that thermal behaviors of metallic glass can be explained in terms of small structural units, especially the glue unit, while deformation requires the atomic operation in a larger scale. The deformation zone includes at least more than one primary cluster of length scale in the order of several nanometers, which is consistent with the scale of shear bands or shear transition zone [25,26]. If breaking of covalent bonds is involved during deformation, the metallic glasses will exhibit brittle behavior. Reduction of percentage of covalent bonds is therefore expected to enhance the plasticity of these systems, as evidenced by recent work [27]. It is therefore interesting to understand the mechanism to reduce the percentage of Fe–B covalent bonding. The tendency to form a certain type of bond can be compared through the heat of mixing between various pairs of elements. The heats of mixing are −26 kJ/mol for Fe–B; −34 kJ/mol for Nb–B; −50 kJ/mol for Y–B; and −71 kJ/mol for Zr–B [28]. These minor constituents bond more readily with B atoms, and likely induce complex structures which favor glass forming. It should also be noted that among all possible bonds with Fe (Fe–Y: −1 kJ/mol, Fe–Zr: −25 kJ/mol, Fe–Nb: −15 kJ/mol) the heat of mixing of Fe–B is the most negative, which indicates that Fe still preferentially bonds with B despite the reduced bonding strength. The covalent bond characters weaken as seen from the broadening of conduction bands and absence of covalent-coupling peak at 9 eV in the FeBM metallic glass. On the other hand, the strong hybridization of Fe 3 d and Zr 4 d in Fe–Zr metallic glasses is also reported to depress the magnetization [29]. Such hybridization delocalizes the Fe 3 d electrons around the Fermi level. The hybridized 3 d electrons will move away from the Fermi level and likely overlap with the minor band. The reduced electronic density of states at the Fermi level stabilizes the structure [30]. In spite of the negative heat of mixing of B-M, strong covalent bonds were not formed between B and the metallic alloying elements. This may also be attributed to the strong hybridization between M *4d* and Fe *3d* electrons. It provides a sound explanation for the dramatic change of mechanical behaviors with the replacement of Si by the metallic alloying elements [31].

4. Conclusions

Significant differences in structural, thermal, mechanical and magnetic properties were revealed between two Fe-based metallic glasses. The dramatic changes can be attributed to the more negative heat of mixing between B and the metallic alloying elements, so that the Fe–B covalent-like bonds were replaced with weaker B-M bonds and destroyed the strong SRO. The results were discussed based on electronic structures and shed lights on methods for designing Fe-based metallic glasses with a combination of high GFA and desirable properties.

Acknowledgements

The work was supported by National Key R&D Program of China (Grant No. 2016YFE0204200) and also partially supported by a grant from the Research Grants Council of the Hong Kong Special Administrative Region, China [(RGC Project No.) CityU 11253716]. Dr. Yingmin Wang also acknowledges the financial support by the National Science Foundation of China (No. 51671045). Dr. Guangcun Shan would like to thank Prof. C.T. Liu for helpful discussions during his visiting as a senior research associate at CityU in 2016. The authors would like to thank beamline BL14B1 (Shanghai Synchrotron Radiation Facility) for providing the beam time and helps during experiments.

References

[1] M. Ohta, Y. Yoshizawa, Appl. Phys. Lett. 91 (2007), 062517.
[2] W.H. Wang, C. Dong, C.H. Shek, Mater. Sci. Eng. R 44 (2004) 45–89.
[3] T. Bitoh, A. Makino, A. Inoue, Mater. Trans., JIM 45 (2004) 1219–1223.
[4] Z.P. Liu, C.T. Liu, J.R. Thompson, W.D. Porter, Phys. Rev. Lett. 92 (2004), 245503.
[5] T. Xu, Z.Y. Jian, F.G. Chang, L.C. Zhou, M.J. Shi, M. Zhu, J.F. Xu, Y.Q. Liu, T. Zhang, J. Alloys. Compd. 699 (2017) 92–97.
[6] J.M. Park, J.S. Park, D.H. Kim, J.H. Kim, E. Fleury, J. Mater. Res. 21 (2006) 1019.
[7] P.H. Gaskell, Nature 267 (1978) 484–485.
[8] J.L. Zhang, Y.M. Wang, C.H. Shek, J. Appl. Phys. 110 (2011), 3650244.
[9] G.C. Shan, J.L. Zhang, J. Li, S. Zhang, Z. Jiang, Y.Y. Huang, C.H. Shek, J. Mag. Mag. Mater 352 (2014) 49.
[10] C. Dong, Q. Wang, J.B. Qiang, Y.M. Wang, N. Jing, G. Hang, Y.H. Li, J. Wu, J.H. Xia, J. Phys. D Appl. Phys. 40 (2007) R273.
[11] D.B. Miracle, Nat. Mater. 10 (2004) 697–702.
[12] H.W. Sheng, W.K. Luo, F.M. Alamgir, J.M. Bai, E. Ma, Nature 439 (2006) 419–425.
[13] W.H. Wang, Prog. Mater. Sci. 52 (2007) 540–596.
[14] B. Ravel, M. Newville, J. Synchrotron Radiat. 12 (2005) 537–541.
[15] J.J. Rehr, R.C. Albers, Rev. Mod. Phys. 72 (2000) 621–654.
[16] F.E. Luborsky, J. Reeve, H.A. Davis, H.H. Liebermann, IEEE Trans. Magn. 6 (1982) 1385.
[17] V.G. Harris, S.A. Oliver, J.D. Ayers, B.N. Das, N.C. Koon, Appl. Phys. Lett. 68 (1996) 2073–2075.
[18] D.E. Polk, Acta Metall. 20 (1970) 485–491.
[19] K.F. Kelton, G.W. Lee, A.K. Gangopadhyay, R.W. Hyers, T.J. Rathz, Phys. Rev. Lett. 90 (2003), 195504.
[20] Y. Zhang, K. Hono, A. Inoue, A. Makino, T. Sakurai, Acta Mater. 44 (1996) 1497–1510.
[21] S.R. Nagel, J. Tauc, Phys. Rev. Lett. 35 (1975) 380–383.
[22] C.H. Shek, Y.M. Wang, C. Dong, Mater. Sci. Eng. 291 (2000) 78–85.
[23] J. Hafner, M. Tegze, Ch Becker, Phys. Rev. B 45 (1994) 285–294.
[24] D.J. Joyner, O. Johnson, D.M. Hercules, D.W. Bullett, J.H. Weaver, Phys. Rev. B 24 (1981) 3122–3137.
[25] P.E. Donovan, W.M. Stobbs, Acta Metall. 29 (1981) 1419–1436.
[26] S.G. Mayr, Phys. Rev. Lett. 97 (2006), 195501.
[27] X.J. Gu, S.J. Poon, G.J. Shiflet, M. Widom, Acta Mater. 56 (2008) 88–94.
[28] A. Takeuchi, A. Inoue, Mater. Trans., JIM 46 (2005) 2817–2829.
[29] M. Yu, Y. Kakehashi, H. Tanake, Phys. Rev. B 49 (1994) 352–367.
[30] P. Ravindran, R. Asokamani, Bull. Mater. Sci. 20 (1997) 613–622.
[31] W. Zhang, H. Miao, Y. Li, C. Chang, G. Xie, X. Jia, J. Alloys. Compd. 707 (2017) 57–62.